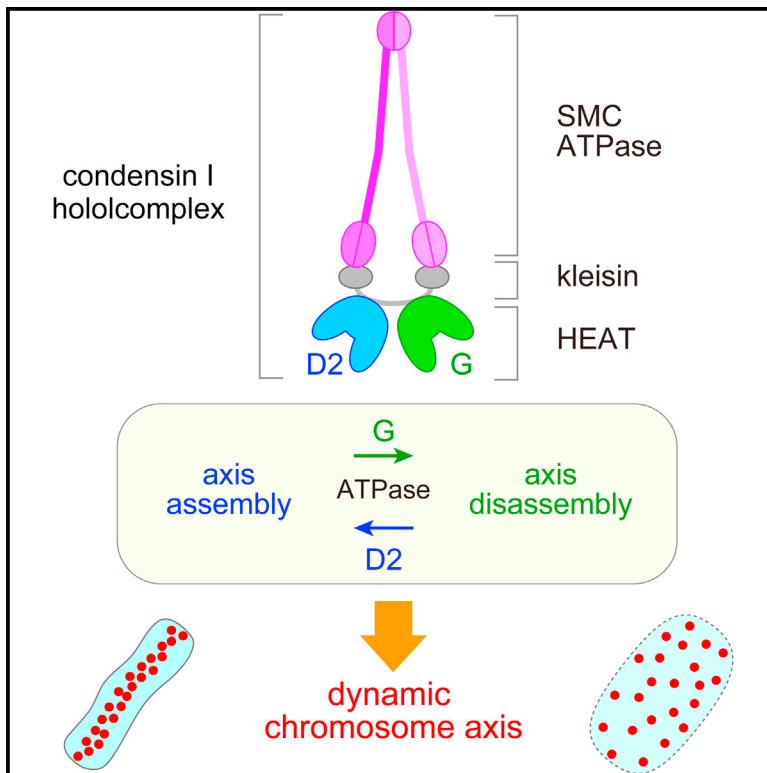


# Developmental Cell

## Balancing Acts of Two HEAT Subunits of Condensin I Support Dynamic Assembly of Chromosome Axes

### Graphical Abstract



### Authors

Kazuhisa Kinoshita, Tetsuya J. Kobayashi, Tatsuya Hirano

### Correspondence

hiranot@riken.jp

### In Brief

The condensin I complex plays a central role in mitotic chromosome assembly and segregation. Kinoshita et al. develop a functional assay for condensin subunits using reconstituted complexes in *Xenopus* egg cell-free extracts, and find, unexpectedly, that the two HEAT subunits have antagonistic effects on the dynamic assembly of chromosome axes.

### Highlights

- An experimental system for dissecting condensin I function is established
- ATP binding and hydrolysis have distinct contributions to condensin I's action
- Continuous ATP hydrolysis is required for maintaining chromosome structure
- Two HEAT subunits have antagonistic functions in chromosome axis assembly



# Balancing Acts of Two HEAT Subunits of Condensin I Support Dynamic Assembly of Chromosome Axes

Kazuhiisa Kinoshita,<sup>1</sup> Tetsuya J. Kobayashi,<sup>2</sup> and Tatsuya Hirano<sup>1,\*</sup>

<sup>1</sup>Chromosome Dynamics Laboratory, RIKEN, 2-1 Hirosawa, Wako, Saitama 351-0198, Japan

<sup>2</sup>Institute of Industrial Sciences, The University of Tokyo, 4-6-1 Komaba, Meguro-ku, Tokyo 153-8505, Japan

\*Correspondence: [hiranot@riken.jp](mailto:hiranot@riken.jp)

<http://dx.doi.org/10.1016/j.devcel.2015.01.034>

## SUMMARY

Condensin I is a five-subunit protein complex that plays a central role in mitotic chromosome assembly and segregation in eukaryotes. To dissect its mechanism of action, we reconstituted wild-type and mutant complexes from recombinant subunits and tested their abilities to assemble chromosomes in *Xenopus* egg cell-free extracts depleted of endogenous condensins. We find that ATP binding and hydrolysis by SMC subunits have distinct contributions to the action of condensin I and that continuous ATP hydrolysis is required for structural maintenance of chromosomes. Mutant complexes lacking either one of two HEAT subunits produce abnormal chromosomes with highly characteristic defects and have contrasting structural effects on chromosome axes preassembled with the wild-type complex. We propose that balancing acts of the two HEAT subunits support dynamic assembly of chromosome axes under the control of the SMC ATPase cycle, thereby governing construction of rod-shaped chromosomes in eukaryotic cells.

## INTRODUCTION

The assembly of rod-shaped chromosomes is one of the most dramatic events occurring during the eukaryotic cell cycle, which was observed by early cytologists in the late 19<sup>th</sup> century (Flemming, 1882). This process is thought to be an essential prerequisite to the separation of sister chromatids at the onset of anaphase and their subsequent partitioning into daughter cells. Despite the long history of chromosome research, mechanistically how chromosomes might be assembled from long DNA molecules and a myriad of associating proteins remains a big mystery. Whereas we have gained substantial knowledge as to the structure of individual nucleosomes, the fundamental unit of eukaryotic chromatin, no consensus is currently available about how the array of nucleosomes might be folded within mitotic chromosomes (Belmont, 2006; Maeshima et al., 2010).

Whatever the possible folding processes, studies during the two past decades or so have demonstrated that condensin I is most likely to be the central player in the process of mitotic chromosome assembly (Hirano, 2012). The five-subunit condensin I

complex was originally identified in *Xenopus* egg cell-free extracts and has later been shown to be conserved from yeast to humans. At its core, a pair of structural maintenance of chromosomes (SMC) subunits (SMC2 and SMC4) forms a V-shaped dimer in which two ATP-binding head domains are located at its distal ends. The third subunit (CAP-H), which belongs to a protein family known as kleisins (Schleiffer et al., 2003), bridges the SMC head domains (Onn et al., 2007). The kleisin subunit is then bound by the remaining two subunits (CAP-D2 and CAP-G), both of which contain HEAT repeats, a motif found in many eukaryotic proteins with diverse functions, including importin  $\beta$  and the A subunit of protein phosphatase 2A (Neuwald and Hirano, 2000). The tandemly repeated HEAT motifs form a highly elastic, solenoidal shape whose conformation drastically changes depending on binding partners or environments (Forwood et al., 2010; Grinthal et al., 2010). The HEAT subunits are unique to eukaryotic condensins, although the basic architecture of SMC-kleisin is largely conserved among bacterial condensins. Thus, it is of great interest how the HEAT subunits might contribute to condensin functions and affect the architecture of eukaryotic chromosomes.

Previous biochemical studies have identified several molecular activities associated with purified condensin I or SMC dimer, including ATP-dependent positive supercoiling of double-stranded DNA (Hagstrom et al., 2002; Kimura and Hirano, 1997; St-Pierre et al., 2009) and reannealing of single-stranded DNA (Sutani and Yanagida, 1997). Evidence is also available that condensin I, like cohesin, has the ability to embrace a DNA strand(s) within its coiled-coil arms (Cuylen et al., 2011). Although these activities illuminate the potential mechanism of action of condensins, there remains a sizable gap between the biochemical assays using purified components and the actual reaction of chromosome assembly taking place under physiological conditions.

In the current study, we attempt to fill the gap by establishing powerful functional assays in which *Xenopus* egg cell-free extracts were combined with a panel of condensin I complexes reconstituted from its recombinant subunits. To address the role of the SMC ATPase cycle, we have reconstituted two different types of mutants defective in either ATP binding or ATP hydrolysis. Our results show that ATP binding and hydrolysis by the SMC subunits have distinct contributions to condensin I functions. We have also reconstituted a panel of subcomplexes that lack the non-SMC regulatory subunits one by one, demonstrating that the two HEAT subunits have apparently antagonistic functions in chromosome axis assembly. Based on these results, we propose that intricate balancing acts of the pair of the HEAT

subunits, being coupled with the SMC ATPase cycle, play a crucial role in building and maintaining rod-shaped chromosomes in eukaryotic cells.

## RESULTS

### ATP Binding and Hydrolysis by SMC Subunits Are Both Essential for Chromosome Assembly

We previously reported a reconstitution of human condensin complexes from recombinant subunits using a baculovirus expression system (Onn et al., 2007). However, expression of the SMC subunits was very poor, making it difficult to reconstitute and purify holocomplexes with a good yield. We therefore decided to redesign the expression constructs by using a different source of mammalian cDNAs. We found that co-insertion of mouse cDNAs for SMC2 and SMC4 into a single vector greatly improved the expression level of these subunits and modified protocols allowed us to obtain the five-subunit holocomplex of condensin I with an excellent yield (Figure 1A). The resulting complex was a chimera of two mouse subunits (mSMC2 and mSMC4) and three human subunits (hCAP-D2, -G, -H). We then tested the ability of the recombinant holocomplex to assemble chromosomes in *Xenopus* egg cell-free extracts. In this experimental system, sperm chromatin was directly incubated with metaphase extracts to assemble a cluster of single-chromatid structures (Hirano and Mitchison, 1994). Figure 1B (upper) shows an example assembled in control extracts. As expected, the cluster of chromosomes was labeled with an antibody against *Xenopus* SMC2 (xSMC2), but not with an antibody against mSMC4. When endogenous condensins were depleted (see Figure S1A for immunoblotting), the extract lost its ability to assemble individual chromosomes (Figure 1B, middle). Neither of the antibodies labeled the fuzzy mass of chromatin formed in this extract. We found that addition of the recombinant condensin I complex into the depleted extract efficiently restored its ability to assemble individual chromosomes (Figure 1B, lower). The structure assembled in this complemented extract was positive for mSMC4 but not for xSMC2. These results demonstrated that the recombinant holocomplex of condensin I is fully functional in this particular assay (Note that because the functional contribution of condensin II is very minor in this cell-free assay [Ono et al., 2003; Shintomi and Hirano, 2011], the addition of recombinant condensin I into extracts depleted of both condensins is sufficient to assemble single chromatids.)

We next wished to test how the ATP-binding and hydrolysis cycle of SMC subunits might modulate condensin I. The ATP-binding “head” domains of SMC ATPases resemble the nucleotide-binding domains of ATP-binding cassette (ABC) transporters. The postulated ATPase cycle of SMC proteins is summarized in Figure 1C. In brief, Walker A (WA) mutations block the step of ATP binding (Hirano et al., 2001), whereas transition-state (TR) mutations stabilize head-head engagement by slowing down the rate of ATP hydrolysis (Hirano and Hirano, 2004). We introduced the corresponding mutations into both SMC subunits (WA, mSMC2 [K38I] and mSMC4 [K117I]; TR, mSMC2 [E1114Q] and mSMC4 [E1218Q]), and reconstituted two mutant complexes accordingly (Figure 1D). Unlike the wild-type holocomplex (hereafter referred to as holo[WT]), which was fully

competent for supporting chromosome assembly in a condensin-depleted extract (Figure 1E, upper), the Walker A mutant complex (holo[WA]) failed to associate with chromatin (Figure 1E, middle). Not surprisingly, no individual chromosomes were formed in this extract (Figures 1E and 1F). The transition-state mutant complex (holo[TR]) also failed to assemble chromosomes, although its loading onto chromatin was readily detectable (Figure 1E, lower; Figure 1F). These results indicated that not only ATP binding, but also hydrolysis is required for proper functions of condensin I.

### Continuous ATP Hydrolysis Is Essential for Structural Maintenance of Chromosomes

To assess the dynamics of condensin I in the egg extracts, we prepared differentially tagged versions of the holocomplex in which the CAP-H subunits was fused with either mCherry or EGFP (Figure 2A, upper; Figure S1B), and set up the following experiments (Figure 2A, lower). In this “sequential add-back” assay, mCherry-tagged condensin I (first complex) was mixed with a condensin-depleted extract, and preincubated for 30 min. Sperm chromatin was then added into this extract and incubated for another 120 min to assemble mitotic chromosomes. Finally, this assembly mixture was mixed with EGFP-tagged condensin I (second complex) that had been preincubated with another condensin-depleted extract. Aliquots were taken at 0, 10, and 30 min after incubation, fixed, and processed for immunofluorescence analyses. We reasoned that, if a chromosome-bound pool of condensin I was continuously exchanged with an unbound pool present in the extract, the EGFP-tagged version would efficiently be incorporated into the chromosomes.

In the first set of experiments, we tested the combination of holo(WT)<sup>mCherry</sup> and holo(WT)<sup>EGFP</sup> (Figure 2B). It was confirmed that holo(WT)<sup>mCherry</sup> was competent for supporting mitotic chromosome assembly as the untagged version of holo(WT) complex (Figure 2B, 0'). As expected, the structure was positive for mCherry but negative for EGFP. Ten minutes after addition of holo(WT)<sup>EGFP</sup>, weak EGFP signals appeared on chromosomes (Figure 2B, 10'). Thirty minutes after addition, the signals became stronger (Figure 2B, 30'), indicating that the subsequently added condensin I complexes were efficiently incorporated into the preassembled chromosomes.

Next we repeated the same experiments using the combination of holo(TR)<sup>mCherry</sup> and holo(TR)<sup>EGFP</sup> (Figure 2C). Like the untagged version of holo(TR), holo(TR)<sup>mCherry</sup> associated with chromatin but failed to assemble individual chromosomes. When holo(TR)<sup>EGFP</sup> was added into the assembly mixture, only faint signals of EGFP were detectable even after 30 min incubation, indicating that the TR mutant complexes were incorporated very slowly compared to the wild-type complexes.

In the final set of experiments, we assembled chromosomes with holo(WT)<sup>mCherry</sup> and then added holo(TR)<sup>EGFP</sup> (Figure 2D). Consistent with the results shown in Figure 2C, loading of holo(TR)<sup>EGFP</sup> onto the chromosomes was very slow. Interestingly, however, we noticed that the chromosome structure preassembled with holo(WT)<sup>mCherry</sup> was disrupted over time. Thirty minutes after addition of holo(TR)<sup>EGFP</sup>, either clear axial structure or individual chromosomes were no longer observed. Thus, even a very small amount of holo(TR) had a strong dominant-negative effect over holo(WT). When the order of addition was reversed,

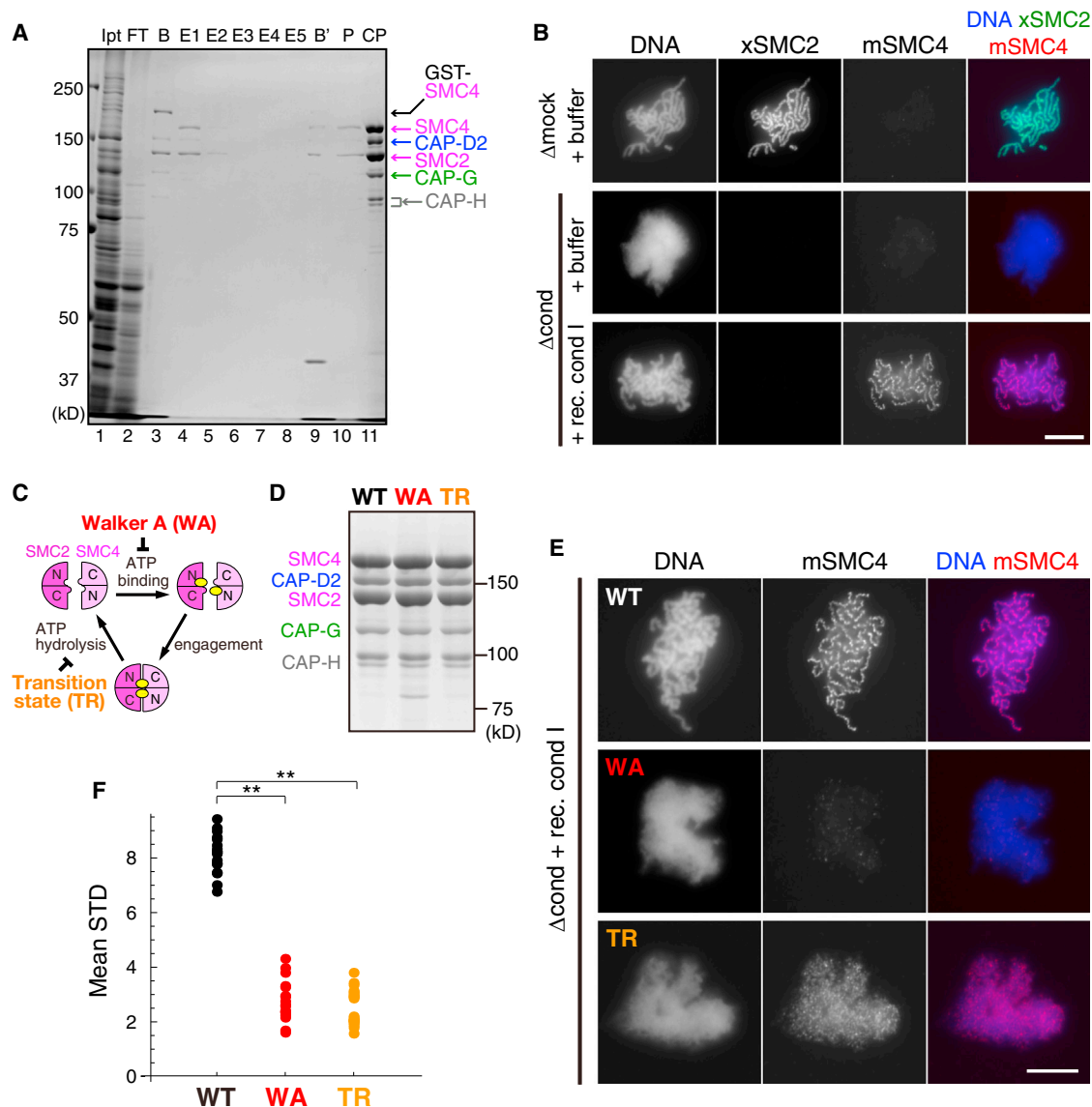


**Figure 1. ATP Binding and Hydrolysis by Condensin I Are Both Essential for Chromosome Assembly in *Xenopus* Egg Extracts**

(A) Purification of the condensin I complex reconstituted from recombinant subunits. The five subunits of condensin I were co-expressed in insect cells, and GST-tagged reconstituted complexes were purified through glutathione affinity chromatography. Protein samples at each step were subjected to SDS-PAGE, and the gel was stained with CBB (lane 1, input [Ipt]; lane 2, flow-through [FT] fraction of glutathione Sepharose beads; lane 3, bead-bound [B] fraction; lanes 4–8, eluted [E1–E5] fractions; lane 9, fraction left on beads after elution [B']; lane 10, pooled fraction [P = E1+E2]; lane 11, pooled fraction after concentration [CP]).

(B) Add-back assay. Mitotic chromosomes were assembled by incubating sperm chromatin with mock-depleted ( $\Delta$ mock) extracts (top), or condensin-depleted ( $\Delta$ cond) extracts supplemented with control buffer (middle) or with the recombinant condensin I complex (bottom). Each sample was fixed and doubly labeled with antibodies against xSMC2 (green) and mSMC4 (red) to depict the endogenous *Xenopus* condensin and the recombinant mammalian condensin I complexes, respectively. DNA was counterstained with DAPI (blue). The data from a single representative experiment out of two repeats are shown. In the experiment shown here, all of the mock-depleted samples ( $n = 19$ ) displayed well-formed chromosomes positive for xSMC2, whereas none of the condensin-depleted samples ( $n = 23$ ) did. One hundred percent of the samples supplemented with recombinant condensin I ( $n = 13$ ) displayed well-formed chromosomes, which were positive for mSMC4 and negative for xSMC2. Scale bar represents 10  $\mu$ m.

(C) A schematic view of the SMC ATPase cycle. Two ATP molecules are sandwiched between the head domains of the SMC2 and SMC4 subunits. Engagement of the ATP-bound head domains triggers ATP hydrolysis, leading to their disengagement. Walker A (WA) mutations block the step of ATP binding, whereas transition-state (TR) mutations slow down the rate of ATP hydrolysis.

(D) The wild-type (WT) and two ATPase mutant (WA and TR) complexes were reconstituted and subjected to SDS-PAGE. The gel was stained with CBB.

(E) Add-back assay. Condensin-depleted extracts were supplemented with the wild-type (WT) and ATPase mutant (WA and TR) complexes, and their abilities to assemble chromosomes were analyzed as in (B). Each sample was labeled with the mSMC4 antibody to depict the recombinant complexes supplemented (red). DNA was counterstained with DAPI (blue). The data from a single representative experiment out of two repeats are shown. In the experiment shown here, all of the

(legend continued on next page)

subsequently added holo(WT)<sup>EGFP</sup> failed to convert the chromatin mass produced with holo(TR)<sup>mCherry</sup> into chromosomes (Figure S2). Taken together, we conclude that continuous ATP hydrolysis not only supports turnover of condensin I, but also is essential for structural maintenance of chromosomes.

### Two HEAT Subunits Have Distinct Functions in Mitotic Chromosome Assembly

One of the biggest advantages of our experimental system is that we can reconstitute a panel of subcomplexes that lack the regulatory subunits one by one. Based on the subunit geometry of condensin I reported in the previous study (Onn et al., 2007), four different subcomplexes were reconstituted and purified (Figures 3A and 3B). Among them, two tetramers that lack either one of the HEAT subunits (CAP-D2 and CAP-G) were referred to as  $\Delta$ D2 and  $\Delta$ G, respectively, whereas a trimer lacking both HEAT subunits was termed  $\Delta$ D2 $\Delta$ G.

We found that none of these subcomplexes has the ability to support proper assembly of mitotic chromosomes in *Xenopus* egg extracts depleted of condensins (Figure 3C; see Figures S3A and S3B for quantitative analyses of chromosome morphology). For instance, the SMC2-4 dimer or the  $\Delta$ D2 $\Delta$ G trimer associated poorly or only weakly with chromatin, failing to induce substantial structural changes in chromatin. In the current study, we hereafter focus on the two tetramers lacking either one of the HEAT subunits, and investigate the distinct defective phenotypes they produced in chromosome assembly. The  $\Delta$ D2 tetramer bound to chromatin in a punctate manner: it failed to produce clearly discernible chromosomes although subtle conformational changes of chromatin were detectable. In striking contrast, the  $\Delta$ G tetramer produced abnormal chromosome structures with highly characteristic properties. As judged by DAPI stain, each chromosome had a DNA-dense axial structure, which was surrounded by a mass of chromatin with a fuzzy surface. Even more striking was that the SMC4 signals were highly concentrated on the axial structures and virtually undetectable in the surrounding regions (Figure 3D). The differences between the wild-type and  $\Delta$ G chromosomes were further confirmed by line scanning of the fluorescence signals (Figure 3D, graph). For further comparison between the two types of chromosomes, see Figures S3C and S3D.

### Highly Unusual Properties of the $\Delta$ G Tetramer and Its Resulting Chromosome Structures

To gain further insights into the axes assembled with the  $\Delta$ G tetramer, we examined the distribution of other chromosomal proteins in the unusual structures. In chromosomes assembled with the holocomplex, topoisomerase II $\alpha$  (topo II $\alpha$ ) was distributed relatively uniformly along chromosomes (Figure 4A). In the  $\Delta$ G chromosomes, a fraction of topo II $\alpha$  was clearly enriched in the abnormal axis structures, whereas it was also readily detectable in the non-axis regions. This is in contrast with the distribution of the  $\Delta$ G tetramer, which was largely undetectable in the

non-axis regions but concentrated on the axes. On the other hand, the distribution of the linker histone B4 and a core histone (as judged by the H3S10ph epitope) were very similar to DAPI-staining patterns (Figure 4B), indicating that histones are present in both axes and non-axis regions.

To further contrast the functional property of the  $\Delta$ G tetramers with that of the holocomplex or  $\Delta$ D2 tetramer, we attempted to assemble mitotic chromosomes under non-standard conditions. We found that the holocomplex was still able to support assembly of individual chromosomes at a high KCl concentration of  $\sim$ 185 mM (the standard KCl concentration was  $\sim$ 100 mM), although they displayed a poor morphology (Figure 4C, upper). The  $\Delta$ D2 tetramer produced some fibrous structures, but displayed no sign of formation of individual chromosomes as judged by SMC4 labeling (Figure 4C, middle). Surprisingly, the  $\Delta$ G tetramer produced a completely different structure under this particular condition (Figure 4C, lower). Whereas sperm chromatin partially swelled, subsequent structural changes were blocked, resulting in formation of a sickle-shaped chromatin mass in which no individual chromatin fibers were discernible. Even more striking was the distribution of the  $\Delta$ G tetramer, which was found to be concentrated into the core of the sickle-shaped structure. Thus, the non-standard assembly reactions provide an additional line of evidence that the two HEAT subunits make distinct contributions to chromosome assembly in this cell-free assay.

### A Subcomplex Lacking CAP-G Is Preferentially Recruited to Preassembled Axes and Elongates Their Structure

To gain more information about the functional properties of the  $\Delta$ G tetramer, we used this subcomplex in sequential add-back assays. In the first set of experiments, we assembled mitotic chromosomes with  $\Delta$ G(WT)<sup>mCherry</sup> and then added holo(WT)<sup>EGFP</sup> (Figure 5A). At 10 min after addition, holo(WT)<sup>EGFP</sup> became detectable on the  $\Delta$ G chromosomes very uniformly. Interestingly, the thin axes that had been produced by the action of  $\Delta$ G(WT)<sup>mCherry</sup> were apparently disassembled at least in part at this time point. By 30 min after addition, the distributions of  $\Delta$ G(WT)<sup>mCherry</sup> and holo(WT)<sup>EGFP</sup> largely overlapped with each other, and the chromosome structures now displayed a morphology similar to that produced with the holocomplex alone. These results suggest that the abnormal chromosomes produced by  $\Delta$ G are not irreversible structures and can be “fixed” by subsequent addition of the holocomplex.

In the second set of experiments, the order of addition was reversed: we first assembled chromosomes with holo(WT)<sup>mCherry</sup> and then added  $\Delta$ G(WT)<sup>EGFP</sup> (Figure 5B). We found that the subsequent addition of  $\Delta$ G(WT)<sup>EGFP</sup> clearly altered the chromosome structure although only a very small amount of  $\Delta$ G(WT)<sup>EGFP</sup> was loaded even at 30 min after addition (see Figure S4A for additional characterization of  $\Delta$ G(WT)<sup>mCherry</sup> and  $\Delta$ G(WT)<sup>EGFP</sup>). The chromosome axes were progressively extended lengthwise and became thinner. Figure 5C shows a close-up view of the

WT samples (n = 17) displayed well-formed chromosomes positive for mSMC4, whereas none of the WA samples (n = 20) did. One hundred percent of the TR samples (n = 26) were positive for mSMC4, but failed to form chromosomes. Scale bar represents 10  $\mu$ m.

(F) For quantification of chromosome morphology as judged by the DAPI-stained images shown in (E), the SD filter was applied to the images after removing background that was estimated by average filtering of the original images. For each sample, the representative value of the STD filter was obtained by averaging the STD values of all pixels within the chromatin area. \*\*p < 0.01 by Mann-Whitney U test.



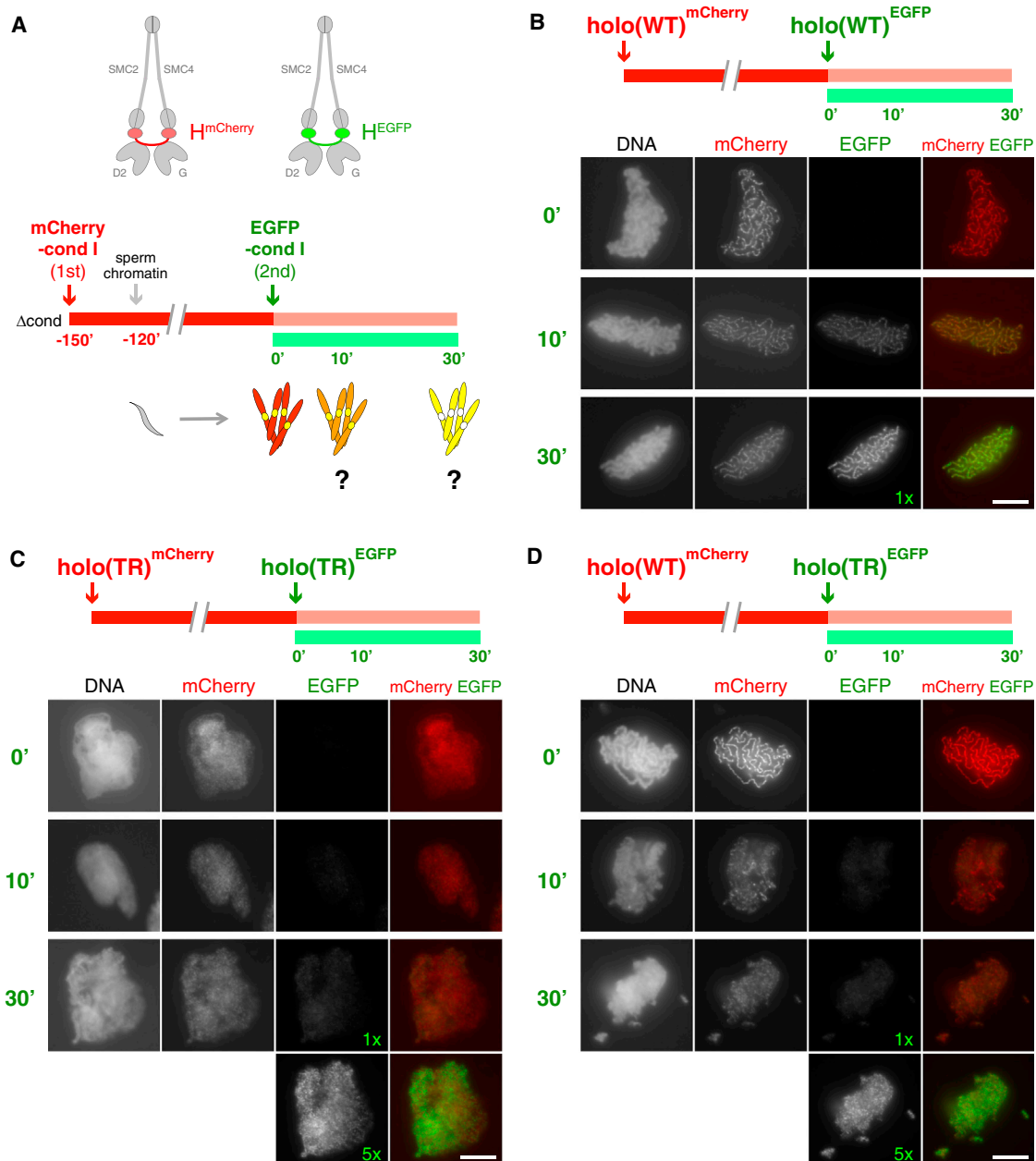


**Figure 2. Continuous ATP Hydrolysis Is Essential for Structural Maintenance of Chromosomes**

(A) Sequential add-back assay using differentially tagged versions of condensin I holocomplexes (holo). A condensin-depleted extract was supplemented with mCherry-tagged condensin I (first) at time -150', and preincubated for 30 min. Sperm chromatin was then added at time -120' and incubated for another 120 min to assemble mitotic chromosomes. EGFP-tagged condensin I (second) was then added at time 0'. Aliquots were taken at time intervals, fixed, and processed for immunofluorescence.

(B) holo(WT)<sup>mCherry</sup> and holo(WT)<sup>EGFP</sup> were used as the first and second complexes, respectively. A representative sample from each time point is shown here (n = 20, 18, and 18 for time 0', 10', and 30', respectively).

(C) holo(TR)<sup>mCherry</sup> and holo(TR)<sup>EGFP</sup> were used as the first and second complexes, respectively. Bottom: to depict the low level of holo(TR)<sup>EGFP</sup> loaded at time 30', the EGFP signals were enhanced by five times longer exposure (5x) compared with the image shown in (B). A representative sample from each time point is shown here (n = 17, 17, and 23 for time 0', 10', and 30', respectively).

(D) holo(WT)<sup>mCherry</sup> and holo(TR)<sup>EGFP</sup> were used as the first and second complexes, respectively. Bottom: the EGFP signals at time 30' were enhanced by five times longer exposure (5x) compared with the image shown in (B). A representative sample from each time point is shown here (n = 20, 22, and 20 for time 0', 10', and 30', respectively). Scale bar represents 10  $\mu$ m.

30-min sample with 5-fold enhanced EGFP signals to visualize the small amount of the  $\Delta G(WT)^{EGFP}$  loaded. It was noticed that the incorporated  $\Delta G$  was preferentially found along the axes in a punctate fashion. Additional images showing the effect of subsequently added  $\Delta G$  are provided in Figure S5.

To test whether the “axis elongation” reaction might be regulated by the SMC ATPase cycle, we replaced  $\Delta G(WT)^{EGFP}$  with  $\Delta G(TR)^{EGFP}$  in a sequential add-back assay. Remarkably, unlike  $\Delta G(WT)^{EGFP}$ , subsequently added  $\Delta G(TR)^{EGFP}$  neither associated with chromosomes nor altered the chromosome axes produced by holo(WT)<sup>mCherry</sup> (Figure 5D). Given our observation that holo(TR) displayed a dominant-negative effect over the action of holo(WT) (Figure 2D), this result further supports the idea that CAP-G’s ability to associate with bulk chromatin contributes to negative regulation of chromosome axis assembly (see Discussion). For additional characterization of  $\Delta G(TR)$  and  $\Delta G(WA)$ , see Figure S6.

### A Subcomplex Lacking CAP-D2 Destabilizes Preassembled Axes

Next, we performed sequential addition assays in the combination of the  $\Delta D2$  tetramer and the holocomplex. In the first set of experiments, we assembled mitotic chromosomes with  $\Delta D2(WT)^{mCherry}$  and then added holo(WT)<sup>EGFP</sup>. It was found that the subsequently added holo(WT)<sup>EGFP</sup> was progressively loaded on the  $\Delta D2$  chromosomes with a poor morphology, but failed to “fix” their structures (Figure 6A). In the second set of experiments in which the order of addition was reversed, the subsequently added  $\Delta D2(WT)^{EGFP}$  was loaded slowly on the chromosomes preassembled with holo(WT)<sup>mCherry</sup> (Figure 6B). We noticed that, at 30 min after addition, part of the chromosome axes was disrupted where  $\Delta D2(WT)^{EGFP}$  was most concentrated (Figure 6B, lower, yellow circles). Thus, the action of the  $\Delta D2$  tetramer was strikingly different from that of the  $\Delta G$  tetramer as judged by the sequential add-back assays, too (see Figure S4B for additional characterization of  $\Delta D2(WT)^{mCherry}$  and  $\Delta D2(WT)^{EGFP}$ ).

Finally, we used the same assays to test whether the two different mutant tetramers ( $\Delta G$  and  $\Delta D2$ ) might functionally interact with each other. We found that subsequently added  $\Delta D2(WT)^{EGFP}$  slowly associated with the  $\Delta G$  chromosomes but did not disrupt their axis structures.  $\Delta D2(WT)^{EGFP}$  distributed throughout the whole chromatin and did not overlap with the axis structures in which the  $\Delta G(WT)^{mCherry}$  was enriched (Figure 6C, 30'). When the order of addition was reversed, subsequently added  $\Delta G(WT)^{EGFP}$  failed to form axis structures. Again, the signals of  $\Delta D2(WT)^{mCherry}$  and  $\Delta G(WT)^{EGFP}$  did not overlap with each other in the final structure (Figure 6D, 30'). Thus, although each of the  $\Delta D2$  and  $\Delta G$  tetramers functionally interacts with the holocomplex in different ways, functional crosstalk between the two mutant tetramers, if any, is very limited.

## DISCUSSION

### Establishing Powerful Experimental Systems for Dissecting the Mechanistic Action of Condensins In Vitro

In the current study, we have combined *Xenopus* egg cell-free extracts with a panel of recombinant condensin complexes to

dissect the mechanistic action of condensin I in vitro. It should be emphasized that our cell-free assay has several advantages over conventional genetics or siRNA-based knockdown approaches, especially when the function of individual subunits of a multi-subunit complex is to be addressed. In many organisms, each of the condensin I subunits is essential for cell viability. When a conditional mutation is introduced into individual subunits (or a single subunit is knocked down), the whole complex often gets destabilized (e.g., Savvidou et al., 2005), making it difficult to assess the role of individual subunits in vivo. In our cell-free assay, we deplete the endogenous complexes, and then add-back mutant complexes. In this case, the mutant complexes are stably present in the complemented extracts, allowing us to search for potentially different phenotypes derived from them. Indeed, we find that the two mutant tetramers,  $\Delta D2$  and  $\Delta G$ , display completely distinct defective phenotypes in the chromosome assembly reaction. Furthermore, we have devised sequential add-back assays that use a pair of differentially tagged complexes. These assays enable us to assess not only the exchange of complexes from chromosomes but also the functional crosstalk between two different complexes.

### Role of the SMC ATPase Cycle in Condensin Functions

The current analysis using the holo(WA) mutant complex demonstrates that ATP binding by the SMC subunits is absolutely essential for chromatin targeting of condensin I in our cell-free assay. On the other hand, the hydrolysis-deficient holo(TR) complex is loaded onto chromatin but fails to assemble individual chromosomes. These results indicate that the steps of ATP binding and hydrolysis have distinct contributions to condensin functions. Equally important, our sequential add-back assays demonstrate that the holo(WT) complex, but not holo(TR), turns over rapidly on chromosomes. Remarkably, when holo(TR) was added into chromosomes preassembled with holo(WT), the chromosome structure was disrupted progressively, suggesting that continued ATP hydrolysis by condensin I is essential for structural maintenance of chromosomes even after the assembly process is apparently complete. We consider two possibilities of how holo(TR) might have a dominant-negative effect over holo(WT). First, holo(TR) would bind to chromatin and “freeze” its conformation in an aberrant fashion so that independently loaded holo(WT) could not work properly. Alternatively, holo(TR) would disturb the action of holo(WT) more directly, for instance, by disrupting its ATP-dependent intercomplex interactions. Whatever the mechanism, our current results greatly extend previous studies involving ectopic expression of SMC2 mutants in chicken DT40 cells (Hudson et al., 2008) and fluorescence-recovery-after-photobleaching analyses in HeLa cells (Gerlich et al., 2006).

### Balancing Acts of the Two HEAT Subunits during Chromosome Axis Assembly

Our analysis using mutant subcomplexes uncovers distinct roles of the two HEAT subunits of condensin I in chromosome assembly. In particular, we were surprised to find that the subcomplex lacking CAP-G ( $\Delta G$  tetramer) produces a highly unique chromosome structure in which an abnormally thin axis is surrounded by a fuzzy mass of bulk chromatin. At first sight, the

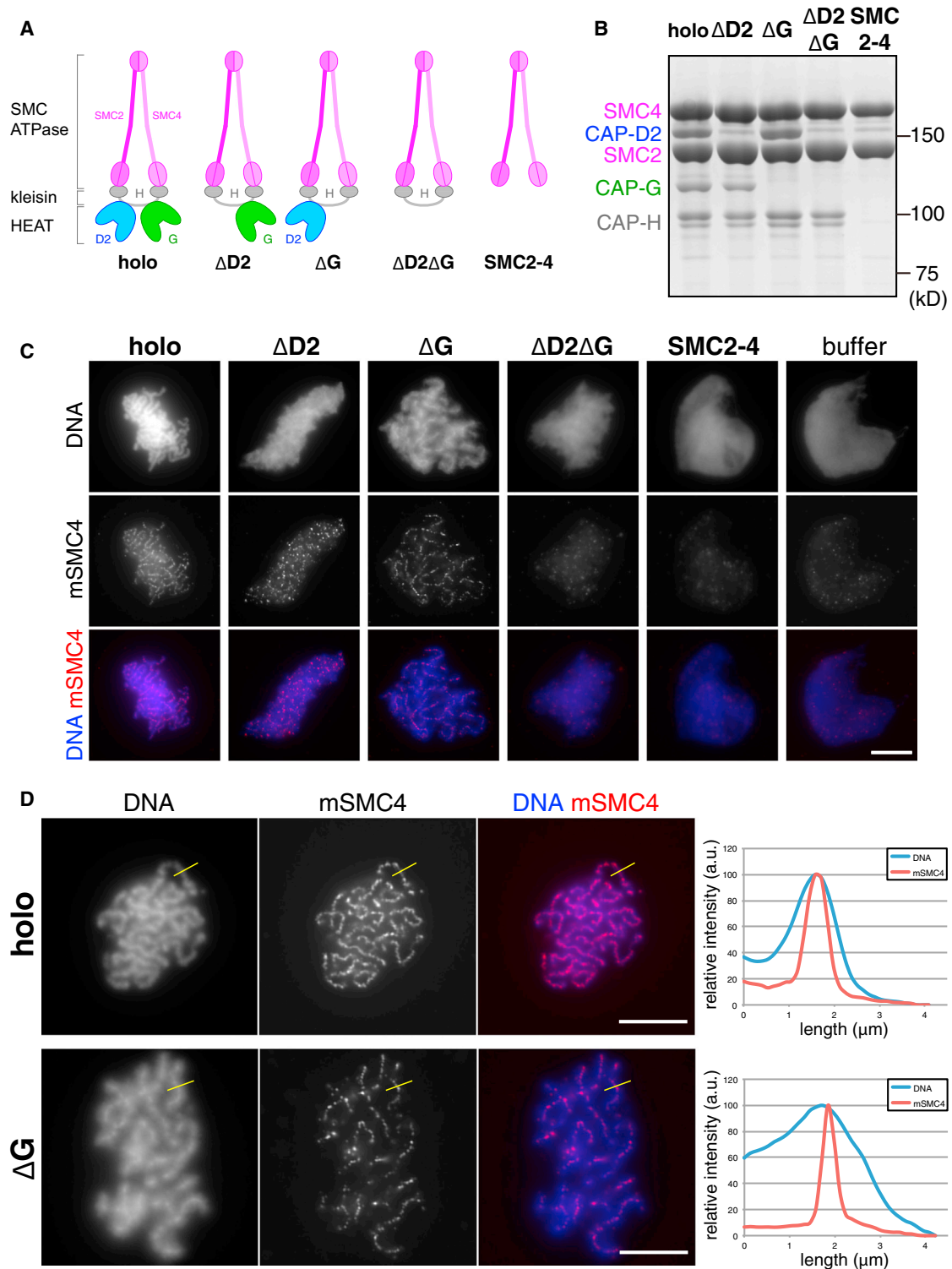


**Figure 3. Two HEAT Subunits Have Distinct Functions in Mitotic Chromosome Assembly**

(A) The holo- and subcomplexes of condensin I reconstituted in the current study. In addition to the five-subunit holocomplex (holo), four different subcomplexes ( $\Delta$ D2 tetramer,  $\Delta$ G tetramer,  $\Delta$ D2 $\Delta$ G trimer, and SMC2-4 dimer) were reconstituted and purified.

(B) Purified holo- and subcomplexes were subjected to SDS-PAGE, followed by staining with CBB.

(C) Add-back assay. Condensin-depleted extracts were supplemented with the holocomplex (holo), the subcomplexes ( $\Delta$ D2,  $\Delta$ G,  $\Delta$ D2 $\Delta$ G, or SMC2-4) or control buffer (buffer), and analyzed as in Figure 1E. Each sample was labeled with antibodies against mSMC4 to depict the recombinant complexes supplemented (red). DNA was counterstained with DAPI (blue). The data from a single representative experiment out of two repeats are shown. In the experiment shown here, multiple

(legend continued on next page)



structure assembled with the  $\Delta G$  tetramer is reminiscent of histone-depleted metaphase chromosomes prepared in a classical series of experiments reported by Laemmli and colleagues (e.g., Paulson and Laemmli, 1977). Unlike the histone-depleted chromosomes, however, the non-axis regions of the  $\Delta G$  chromosomes do contain histones (and topo II), suggesting that intact yet relaxed nucleosome loops radiate from the central axes in these chromosomes.

The current data allow us to propose a model in which the balancing acts of the two HEAT subunits plays a crucial role in dynamic assembly of chromosome axes (Figure 7, i). According to this model, the CAP-D2 subunit plays a primarily role in assembling chromosome axes whereas the CAP-G subunits antagonizes the action of CAP-D2. When the CAP-G subunit is missing, the balance is compromised, resulting in the formation of abnormal chromosomes with thin axes (Figure 7, ii). Conversely, when the CAP-D2 subunit is missing, the  $\Delta D2$  tetramer binds to bulk chromatin but never assembles axes (Figure 7, iii). This model is not contradictory to the recent report that CAP-G is required for condensin I's association with chromosomes in yeast and human cells (Piazza et al., 2014). Functional interactions among these complexes, as revealed by the sequential add-back assays, also provide us with valuable information. Subsequently added holo(WT) reorganizes the unusual axes produced by  $\Delta G$ (WT) (Figure 5A), whereas  $\Delta G$ (WT) effectively elongates the axes preassembled with holo(WT) (Figure 5B; Figure 7, iv). The unique response observed in each experimental setup could reflect different kinetics and different targeting sites between the two complexes. On the other hand,  $\Delta D2$ (WT) has dominant-negative effects, either preventing holo(WT) from assembling normal axes (Figure 6A) or destabilizing the axes preassembled with holo(WT) (Figure 6B; Figure 7, v). Equally important,  $\Delta G$ (WT) and  $\Delta D2$ (WT) bind to and act on chromosomes independently, regardless of the order of addition (Figures 6C and 6D), implicating that the two mutant tetramers do not functionally crosstalk to each other (Figure 7, vi). Thus, to observe functional interplays (either positive or negative) between two different complexes, each of the complexes must contain the same type of HEAT subunits, implicating that intercomplex crosstalks might involve homotypic HEAT-HEAT interactions (i.e., D2-D2 or G-G). Despite substantial efforts, however, we have so far been unsuccessful to obtain evidence for direct and physical interactions among the HEAT subunits. We speculate that the hypothetical HEAT-HEAT interactions might be highly flexible and dynamic ones, which use their spring-like surfaces (Forwood et al., 2010; Grinthal et al., 2010) and are intricately regulated by the SMC ATPase cycle. We also infer that such interactions would occur only on chromosomes, but not in solutions.

### What Are Chromosome Axes?

What might the molecular nature of chromosome axes be? Two pieces of information from the current study shed light on

this long-term question in chromosome biology. First, although  $\Delta G$ (WT) is preferentially recruited to the axes of the holo(WT) chromosomes and elongates them,  $\Delta G$ (TR) does not bind to the same chromosomes at all (Figure 7, vii). Interestingly, this behavior of  $\Delta G$ (TR) is also distinct from that of holo(TR), which binds to and destabilizes the holo(WT) chromosomes (Figure 7, viii). Thus, unlike the holocomplex, the  $\Delta G$  tetramer demands ATP hydrolysis even for its initial interaction with chromosomes, further underscoring the dynamic nature of CAP-D2-mediated axis assembly.

Second, our attempt to assemble chromosomes under high-salt conditions further highlights the usual properties of the  $\Delta G$  tetramer. As discussed above, exposing isolated chromosomes to a high concentration of salt had been one of the classical methods for preparing histone-depleted chromosomes (Lewis and Laemmli, 1982; Paulson and Laemmli, 1977). The resultant "chromosome scaffold" fraction was later shown to contain one of the condensin subunits, SMC2/Sc2 (Saitoh et al., 1994). Similar, if not identical, observations were also made in *Xenopus* cell-free extracts: when an extra concentration of salt is added into preassembled chromosomes, condensin subunits become highly concentrated on their central axis regions (Hirano and Mitchison, 1994; Ono et al., 2003). Although the physiological relevance of these observations has been debated, it seems plausible to hypothesize that an increase in ionic strength induces conformational changes of the hydrophobic core of the HEAT subunits (Kappel et al., 2010) and artificially stabilizes them on axis regions. In the current study, we find unexpectedly that the  $\Delta G$  tetramer makes salt-induced aggregates even during the process of chromosome assembly (see Figure 4C), thereby providing additional insights into the hitherto-enigmatic properties of condensin components as well as the physical nature of chromosome axes.

Finally, it should be added that axis-like structures could also be formed by chromosomal components other than condensins. For instance, a recent paper has reported that unusual axis structures coated with cohesin (termed "vermicelli") become detectable in unduplicated chromosomes when cohesin's dynamics is greatly suppressed in the cell (Tedeschi et al., 2013). Notably, the cohesin complex also has HEAT-containing regulators (Nasmyth and Haering, 2005), raising the possibility that cohesin and condensins might share a common mechanism of action that provides chromosomes with their elastic properties, as predicted by Grinthal et al. (2010).

### Evolutionary Implications

Although protein complexes related to condensins are widely conserved among prokaryotes, it is important to note that the HEAT subunits are unique to eukaryotic condensins (Hirano, 2012). If the HEAT subunits play a crucial role in the assembly of chromosome axes, as proposed in the current study, it is tempting to speculate that acquisition of the HEAT subunits during evolution could have provided condensins with an

images were collected for condensin-depleted extracts supplemented with the holo ( $n = 24$ ),  $\Delta D2$  ( $n = 19$ ),  $\Delta G$  ( $n = 15$ ),  $\Delta D2\Delta G$  ( $n = 11$ ), SMC2-4 ( $n = 12$ ) complexes and buffer ( $n = 13$ ). Scale bar represents 10  $\mu m$ .

(D) Comparison of chromosome axes produced by the  $\Delta G$  tetramer with those assembled by the holocomplex. Each sample was labeled (mSMC4, red) and counterstained (DNA, blue) as in (C). The signal intensities of DNA and mSMC4 were scanned along the yellow lines and plotted. y axis, relative fluorescence intensity of grayscale images (a.u.); x axis, distance along the drawn lines ( $\mu m$ ). Scale bar represents 10  $\mu m$ .

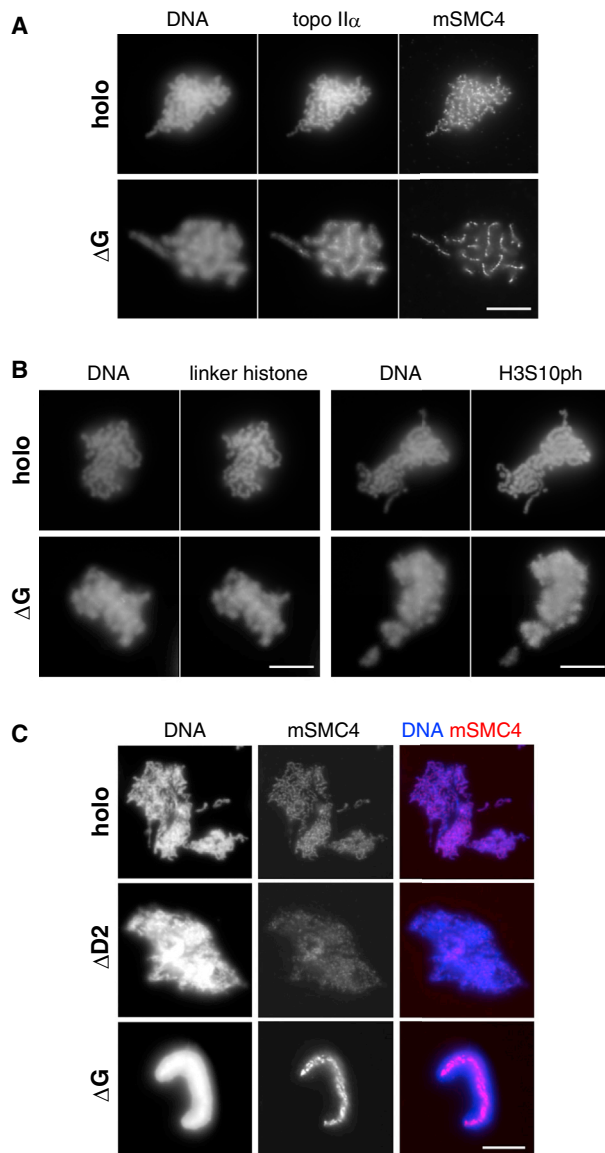


**Figure 4. Further Characterization of Chromosomes Assembled with the  $\Delta G$  Tetramer**

(A) Condensin-depleted extracts were supplemented with the holocomplex and the  $\Delta G$  tetramer, and analyzed by immunofluorescence using antibodies against topoisomerase II $\alpha$  (topo II $\alpha$ ). Each sample was double-labeled with antibodies against topo II $\alpha$  and mSMC4. DNA was counterstained with DAPI. Representative samples are shown here ( $n = 20$  and  $22$  for holo and  $\Delta G$ , respectively). Scale bar represents  $10 \mu m$ .

(B) Chromosomes assembled as in (A) were labeled with antibodies against histones. Samples were labeled with antibodies against linker histone B4 (left) or against histone H3 phospho-Ser10 (H3S10ph, right). Representative samples are shown here (linker histone B4,  $n = 16$  and  $22$  for holo and  $\Delta G$ , respectively; H3S10ph,  $n = 21$  and  $19$  for holo and  $\Delta G$ , respectively). Scale bar represents  $10 \mu m$ .

(C) Condensin-depleted extracts were supplemented with the holocomplex (holo) or the subcomplexes ( $\Delta D2$  or  $\Delta G$ ), and chromosomes were assembled under a non-standard condition with a high concentration of salt ( $185 \text{ mM KCl}$ ). Samples were labeled with antibodies against mSMC4 (red). DNA was counterstained with DAPI (blue). Representative samples are shown here ( $n = 20$ ,  $17$ , and  $29$  for holo,  $\Delta D2$ , and  $\Delta G$ , respectively). Scale bar represents  $10 \mu m$ .

opportunity to build up rod-shaped structures that are unique to eukaryotic chromosomes (see Figure S7). Devising such a new strategy of genome packaging, most likely being coupled with acquisition of nucleosome structures, might have enabled organisms to organize and manipulate a set of linear chromosomes with dramatically increased lengths.

## EXPERIMENTAL PROCEDURES

### Expression and Purification of Recombinant Condensin Subunits

To express condensin subunits in insect cells, we used the Bac-to-Bac Baculovirus Expression System (Life Technologies). Full-length cDNAs for mouse SMC2 (mSMC2, NM\_008017) and SMC4 (mSMC4, NM\_133786) were obtained from the IMAGE Consortium (distributed by Open Biosystems) and subcloned into pFastBac Dual vector to co-express mSMC2 and mSMC4 from a single construct (pFastBac-mSMC2-mSMC4). At the NH<sub>2</sub>-terminus of mSMC4, a GST-tag fused to the 3C protease site was introduced. To construct ATPase mutants of the mSMC2-4 dimer, point mutations were introduced into pFastBac-mSMC2-mSMC4 by using QuikChange II XL Site-Directed Mutagenesis Kit (Agilent Technologies). Primers used for mutagenesis were as follows (mutation sites introduced were underlined): KZ109 (mSMC2 Walker A [K38I]), 5'-GGTAGTGGAAATATCCAACATATTGG-3'; KZ111 (mSMC4 Walker A [K117I]), 5'-GGCAGTGGAAATATCCAATGTTATTG-3'; KZ117 (mSMC2 Transition state [E1114Q]), 5'-CAATTTATATCTTGGATCAGGTGGATGCGG-3'; KZ119 (mSMC4 Transition state [E1218Q]), 5'-CTACTTCATGGATCAGATTGATGCAGC-3'. Constructs for expressing untagged or His-tagged versions of human non-SMC subunits (hCAP-D2, hCAP-G and hCAP-H) were described previously (Onn et al., 2007). For purification of differentially tagged versions of complexes, full-length cDNA for hCAP-H was fused to mCherry or EGFP at its NH<sub>2</sub> terminus and subcloned into pFastBac vector. Bacmid DNAs were prepared according to the manufacturer's instructions and baculoviruses were amplified in Sf9 cells (Life Technologies). To reconstitute holocomplexes or subcomplexes, High Five cells (Life Technologies;  $2\text{--}4 \times 10^8$  cells) were co-transfected with the recombinant viruses in appropriate combinations and were grown at  $29^\circ\text{C}$  for 48 hr. The cells were harvested, resuspended in  $40 \text{ ml}$  of lysis buffer ( $10 \text{ mM K-HEPES}$  [pH 7.7],  $150 \text{ mM KCl}$ ,  $2 \text{ mM MgCl}_2$ ,  $0.1 \text{ mM CaCl}_2$ ,  $5 \text{ mM EGTA}$ ,  $50 \text{ mM sucrose}$ ,  $0.1\%$  Triton X-100, and  $2.5 \text{ U/ml Benzonase}$  [Novagen]), lysed by sonication, and clarified by centrifugation. The clear lysates were supplemented with extra KCl at a final concentration of  $300 \text{ mM}$  and incubated with  $4 \text{ ml}$  of Glutathione Sepharose 4B beads (GE Healthcare) at  $4^\circ\text{C}$  for  $1 \text{ hr}$  to capture complexes containing the GST-tagged mSMC4 subunit. The beads were then packed into a  $5\text{-ml}$  disposable column (QIAGEN) and washed with ice-cold purification buffer ( $10 \text{ mM K-HEPES}$  [pH 7.7],  $300 \text{ mM KCl}$ ,  $2 \text{ mM MgCl}_2$ ,  $0.1 \text{ mM CaCl}_2$ ,  $5 \text{ mM EGTA}$ ,  $50 \text{ mM sucrose}$ , and  $1 \text{ mM DTT}$ ). To remove non-specifically bound heat-shock proteins, the beads were incubated with  $4 \text{ ml}$  of purification buffer (supplemented with  $2 \text{ mM ATP}$  and extra  $8 \text{ mM MgCl}_2$ ) at room temperature for  $20 \text{ min}$ . After being washed with purification buffer again, the beads were treated with PreScission proteases (GE Healthcare) in the purification buffer at  $4^\circ\text{C}$  overnight. Fractions containing released protein complexes were pooled and concentrated with Amicon Ultra-15 (Merck Millipore). Typical yields of complexes purified by this procedure were  $\sim 0.2\text{--}0.5 \text{ mg}$ .

### Preparation of Xenopus Egg Extracts and Immunodepletion

Mitotic high-speed supernatants (HSS) were prepared from *Xenopus* egg extracts made in XBE2 ( $10 \text{ mM K-HEPES}$  [pH 7.7],  $100 \text{ mM KCl}$ ,  $2 \text{ mM MgCl}_2$ ,  $0.1 \text{ mM CaCl}_2$ ,  $5 \text{ mM EGTA}$ , and  $50 \text{ mM sucrose}$ ) as described previously (Hirano et al., 1997). For complete depletion of *Xenopus* endogenous condensins I and II, two rounds of immunodepletion were performed using Dynabeads Protein A (Life Technologies) as described previously (Funabiki and Murray, 2000; Kimura and Hirano, 2000) with the following modifications. A mixture of  $12.5 \mu\text{g}$  of affinity-purified anti-xCAP-D2 or anti-xCAP-G,  $6.25 \mu\text{g}$  of affinity-purified anti-xSMC4 (xCAP-C) and anti-xSMC2 (xCAP-E) was coupled to  $100 \mu\text{l}$  of the beads. The antibody-coupled beads were washed twice with PBS-TX (PBS,  $0.1\%$  Triton X-100) and twice with XBE2. For the first round of depletion,  $100 \mu\text{l}$  of HSS was incubated with the anti-xCAP-D2/xSMC2/xSMC4 beads at  $4^\circ\text{C}$  for  $30 \text{ min}$  on a laboratory rotating wheel. The supernatants were

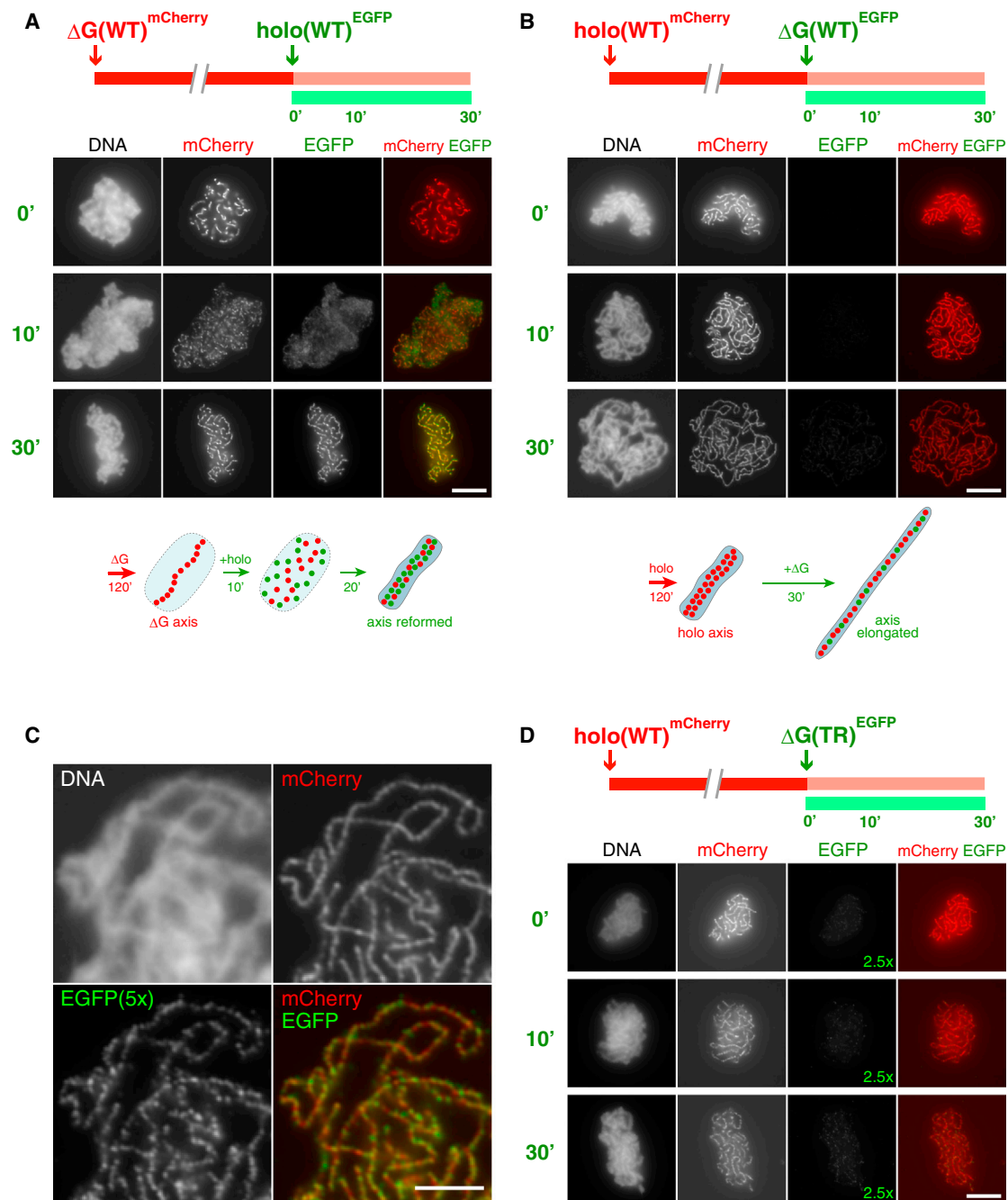


**Figure 5. The  $\Delta G$  Tetramer Is Preferentially Recruited to Chromosome Axes and Elongates Their Structure**

(A) Sequential add-back assay was performed as shown in Figure 2B. mCherry-tagged  $\Delta G(WT)$  and EGFP-tagged holo(WT) were used as the first and second complexes, respectively. A representative sample from each time point is shown here ( $n = 14, 14$ , and  $15$  for time  $0'$ ,  $10'$ , and  $30'$ , respectively). Scale bar represents  $10 \mu m$ .

(B) holo(WT)<sup>mCherry</sup> and  $\Delta G(WT)^{EGFP}$  were used as the first and second complexes, respectively. A representative sample from each time point is shown here ( $n = 23, 25$ , and  $40$  for time  $0'$ ,  $10'$ , and  $30'$ , respectively). Additional images showing the effect of subsequently added  $\Delta G$  are provided in Figure S5.

(C) Close-up images of the  $30'$  sample shown in (B). To depict the low level of  $\Delta G(WT)^{EGFP}$  loaded, the EGFP signals were enhanced by five times longer exposure ( $5\times$ ) compared with the image shown in (B). Scale bar represents  $5 \mu m$ .

(D) holo(WT)<sup>mCherry</sup> and  $\Delta G(TR)^{EGFP}$  were used as the first and second complexes, respectively. The EGFP signals were enhanced by 2.5-times longer exposure ( $2.5\times$ ) compared with the image shown in (A) and (B). A representative sample from each time point is shown here ( $n = 8, 7$ , and  $10$  for time  $0'$ ,  $10'$ , and  $30'$ , respectively). Scale bar represents  $10 \mu m$ .

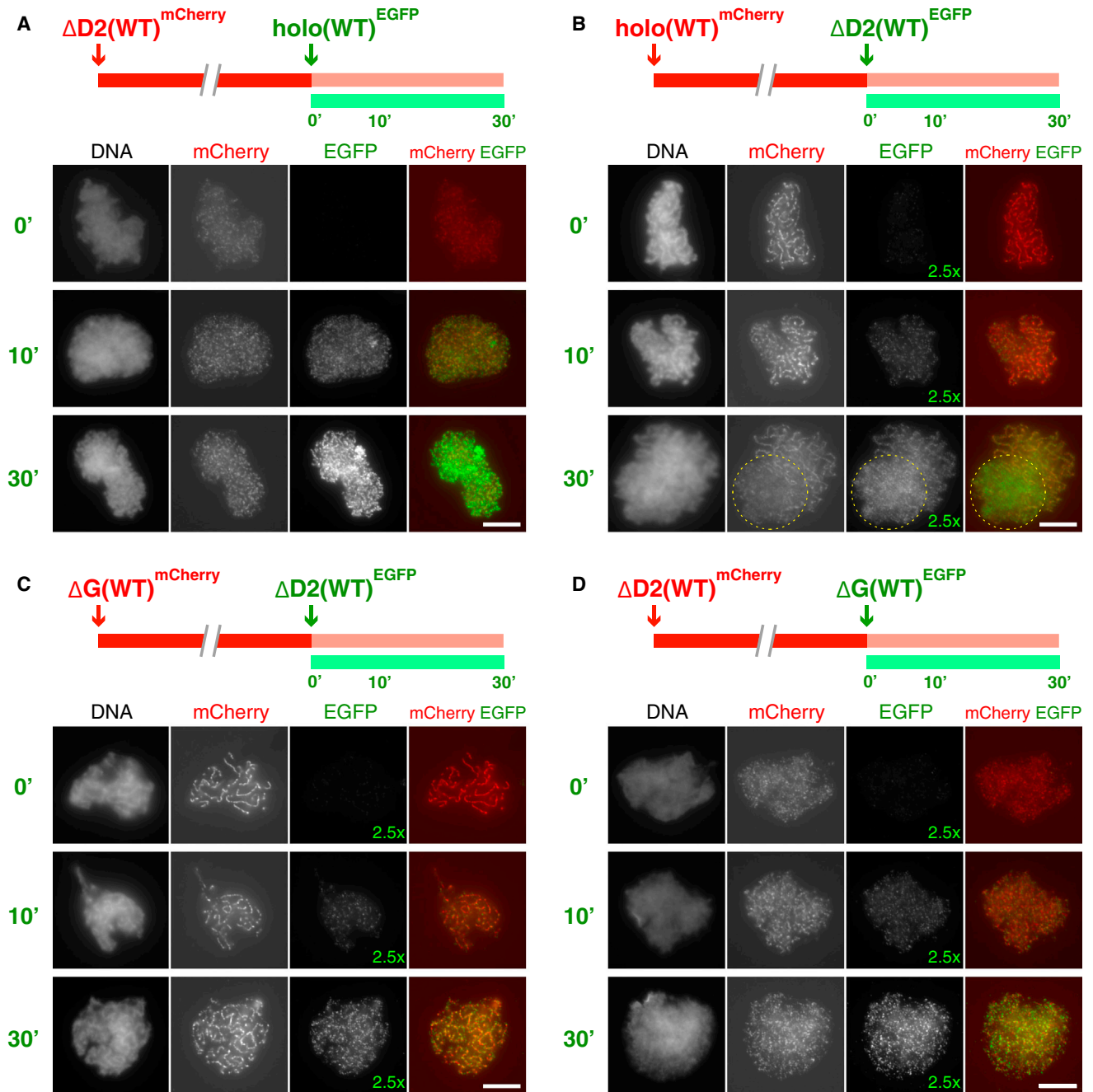


**Figure 6. The  $\Delta D2$  Tetramer Destabilizes Chromosome Axes Assembled with the Holo complex but Not Those Assembled with  $\Delta G$**

(A) Sequential addition assay was performed as shown in Figure 2B. mCherry-tagged  $\Delta D2(WT)$  and EGFP-tagged  $holo(WT)$  were used as the first and second complexes, respectively. A representative sample from each time point is shown here ( $n = 12, 14$ , and  $17$  for time  $0'$ ,  $10'$ , and  $30'$ , respectively).

(B)  $holo(WT)^{mCherry}$  and  $\Delta D2(WT)^{EGFP}$  were used as the first and second complexes, respectively. To depict the low level of  $\Delta D2(WT)^{EGFP}$  loaded, the EGFP signals were enhanced by 2.5-times longer exposure ( $2.5\times$ ) compared with the image shown in (A). A representative sample from each time point is shown here ( $n = 17, 20$ , and  $21$  for time  $0'$ ,  $10'$ , and  $30'$ , respectively).

(C)  $\Delta G(WT)^{mCherry}$  and  $\Delta D2(WT)^{EGFP}$  were used as the first and second complexes, respectively. To depict the low level of  $\Delta D2(WT)^{EGFP}$  loaded, the EGFP signals were enhanced by 2.5-times longer exposure ( $2.5\times$ ) compared with the image shown in (A). A representative sample from each time point is shown here ( $n = 26, 18$ , and  $25$  for time  $0'$ ,  $10'$ , and  $30'$ , respectively).

(D)  $\Delta D2(WT)^{mCherry}$  and  $\Delta G(WT)^{EGFP}$  were used as the first and second complexes, respectively. To depict the low level of  $\Delta G(WT)^{EGFP}$  loaded, the EGFP signals were enhanced by 2.5-times longer exposure ( $2.5\times$ ) compared with the image shown in (A). A representative sample from each time point is shown here ( $n = 13, 13$ , and  $12$  for time  $0'$ ,  $10'$ , and  $30'$ , respectively). Scale bar represents  $10\ \mu m$ .



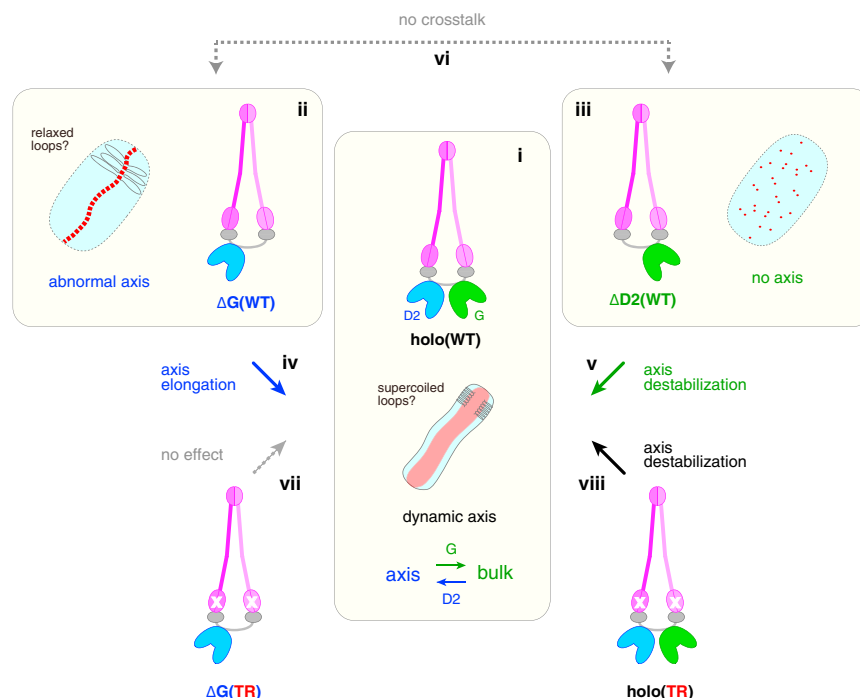


**Figure 7. A Model for Dynamic Assembly of Chromosome Axes by Condensin I**

With the condensin I holocomplex (holo[WT]), balancing acts of the two HEAT subunits (CAP-D2 and CAP-G) support the assembly of chromosomes with dynamic axes (i). CAP-D2 positively acts for axis assembly whereas CAP-G apparently antagonizes the action of CAP-D2. Importantly, ATP binding and hydrolysis are both essential for this assembly reaction. The  $\Delta G$  tetramer ( $\Delta G$ [WT]) produces chromosomes with abnormally thin axes (ii), whereas the  $\Delta D2$  tetramer ( $\Delta D2$ [WT]) produces chromatin masses with no axes (iii). In contrast, addition of  $\Delta G$ (WT) is added into chromosomes preassembled with the holocomplex, it is recruited preferentially to their axes and elongates them (iv). In contrast, addition of  $\Delta D2$ (WT) destabilizes the preassembled axes (v). On the other hand,  $\Delta G$ (WT) and  $\Delta D2$ (WT) do not crosstalk and behave independently (vi). The  $\Delta G$  tetramer with hydrolysis-deficient mutations ( $\Delta G$ [TR]) does not bind to the preassembled chromosomes at all, having little effect on their structure (vii). When the same mutations are introduced into the holocomplex (holo[TR]), the resultant complex binds to the chromosomes and destabilizes their structures (viii).

separated from the beads with magnets, transferred to a new tube, and then subjected to the second round of depletion with the anti-xCAP-G/xSMC2/xSMC4 beads. After incubation at 4°C for 30 min, the supernatants were separated from the magnetic beads and used as condensin-depleted extracts.

#### Chromosome Assembly Assays Using *Xenopus* Egg Extracts

For standard add-back assays, condensin-depleted extracts were supplemented with purified recombinant complexes (16–35 nM) and an energy mix (1 mM MgATP, 10 mM creatine phosphate, and 50  $\mu$ g/ml creatine kinase), and preincubated at 22°C for 30 min. Sperm chromatin was then added at a final concentration for  $1\text{--}2 \times 10^3$  nuclei/ $\mu$ l and incubated for another 120 min to assemble chromosomes. In some experiments, condensin-depleted extracts were mixed with recombinant complexes and sperm chromatin, and incubated at 30°C for 90 min. After incubation, the reaction mixtures were fixed and processed for immunofluorescence analyses as describe below. For sequential add-back assays using differentially tagged versions of recombinant complexes, condensin-depleted extracts were mixed with first complexes containing mCherry-tagged hCAP-H and preincubated at 22°C for 30 min. Sperm chromatin was then added into the mixture and incubated for 120 min to assemble chromosomes. Second complexes containing EGFP-tagged hCAP-H that had also been preincubated with condensin-depleted extracts were added into the mixture at time 0, and incubation was continued for another 30 min. Aliquots were taken at 0, 10, and 30 min, and processed for immunofluorescence analyses.

#### Immunofluorescence Analyses

Immunofluorescence for chromosomes assembled in the extracts was performed as described previously (Ono et al., 2003; Shintomi and Hirano, 2011) with minor modifications. Ten microliters of reaction mixtures were fixed with 100  $\mu$ l of 2% paraformaldehyde in XBE2 containing 0.1% Triton X-100 at room temperature for 10 min, centrifuged onto coverslips, and processed for immunofluorescence. Anti-linker histone B4 antibody was a gift from Dr. Keita Ohsumi (Ohsumi et al., 1993; Shintomi et al., 2005). For double immunolabeling with antibodies against *Xenopus* and mouse condensin subunits, coverslips were first incubated with anti-mSMC4 antibody (Lee et al., 2011), followed by incubation with Alexa Fluor 568-conjugated anti-rabbit IgG (Life Technologies). The coverslips were treated with nonimmune rabbit IgG (at a final concentration of 0.5  $\mu$ g/ $\mu$ l) to saturate open IgG-binding sites in

the secondary antibody, and then incubated with biotin-labeled anti-xSMC2 antibody, followed by incubation with Alexa Fluor 488 streptavidin conjugates (Life Technologies). For the sequential add-back assays, rabbit antibodies against GFP (MBL) and mouse antibodies against mCherry (Clontech) were used for detection of the tagged subunits. After counterstaining with DAPI, the coverslips were mounted on slides with Vectashield mounting medium (Vector Laboratories) and examined with an Olympus BX51 microscope equipped with a cooled charge-coupled device camera. Grayscale images were pseudocolored and merged by using Photoshop (Adobe). For measurement of the signal intensity of DNA and mSMC4, the immunofluorescence signals on the scanned line were quantified by using the plot profile function of the ImageJ software (<http://imagej.nih.gov/ij/>). The details of quantification of chromosome morphology are described in the [Supplemental Experimental Procedures](#).

#### SUPPLEMENTAL INFORMATION

Supplemental Information includes Supplemental Experimental Procedures and seven figures and can be found with this article online at <http://dx.doi.org/10.1016/j.devcel.2015.01.034>.

#### AUTHOR CONTRIBUTIONS

K.K. and T.H. designed research; K.K. performed all the experiments; T.J.K. performed image analyses; K.K. and T.H. wrote the manuscript.

#### ACKNOWLEDGMENTS

We thank K. Ohsumi for anti-B4 antibody, A. Matsuura for technical assistance, and members of the Hirano lab for critically reading the manuscript. This work was supported by Grant-in-Aid for Scientific Research C (to K.K.), and Grant-in-Aid for Specially Promoted Research (to T.H.).

Received: August 10, 2014

Revised: October 16, 2014

Accepted: January 29, 2015

Published: April 6, 2015



## REFERENCES

- Belmont, A.S. (2006). Mitotic chromosome structure and condensation. *Curr. Opin. Cell Biol.* **18**, 632–638.
- Cuylen, S., Metz, J., and Haering, C.H. (2011). Condensin structures chromosomal DNA through topological links. *Nat. Struct. Mol. Biol.* **18**, 894–901.
- Flemming, W. (1882). *Zellsubstanz, Kern und Zelltheilung* (Leipzig, Germany: F.C.W. Vogel).
- Forwood, J.K., Lange, A., Zachariae, U., Marfori, M., Preast, C., Grubmüller, H., Stewart, M., Corbett, A.H., and Kobe, B. (2010). Quantitative structural analysis of importin- $\beta$  flexibility: paradigm for solenoid protein structures. *Structure* **18**, 1171–1183.
- Funabiki, H., and Murray, A.W. (2000). The *Xenopus* chromokinesin Xkid is essential for metaphase chromosome alignment and must be degraded to allow anaphase chromosome movement. *Cell* **102**, 411–424.
- Gerlich, D., Hirota, T., Koch, B., Peters, J.M., and Ellenberg, J. (2006). Condensin I stabilizes chromosomes mechanically through a dynamic interaction in live cells. *Curr. Biol.* **16**, 333–344.
- Grinthal, A., Adamovic, I., Weiner, B., Karplus, M., and Kleckner, N. (2010). PR65, the HEAT-repeat scaffold of phosphatase PP2A, is an elastic connector that links force and catalysis. *Proc. Natl. Acad. Sci. USA* **107**, 2467–2472.
- Hagstrom, K.A., Holmes, V.F., Cozzarelli, N.R., and Meyer, B.J. (2002). *C. elegans* condensin promotes mitotic chromosome architecture, centromere organization, and sister chromatid segregation during mitosis and meiosis. *Genes Dev.* **16**, 729–742.
- Hirano, T. (2012). Condensins: universal organizers of chromosomes with diverse functions. *Genes Dev.* **26**, 1659–1678.
- Hirano, M., and Hirano, T. (2004). Positive and negative regulation of SMC-DNA interactions by ATP and accessory proteins. *EMBO J.* **23**, 2664–2673.
- Hirano, T., and Mitchison, T.J. (1994). A heterodimeric coiled-coil protein required for mitotic chromosome condensation in vitro. *Cell* **79**, 449–458.
- Hirano, T., Kobayashi, R., and Hirano, M. (1997). Condensins, chromosome condensation protein complexes containing XCAP-C, XCAP-E and a *Xenopus* homolog of the *Drosophila* Barren protein. *Cell* **89**, 511–521.
- Hirano, M., Anderson, D.E., Erickson, H.P., and Hirano, T. (2001). Bimodal activation of SMC ATPase by intra- and inter-molecular interactions. *EMBO J.* **20**, 3238–3250.
- Hudson, D.F., Ohta, S., Freisinger, T., Macisaac, F., Sennels, L., Alves, F., Lai, F., Kerr, A., Rappsilber, J., and Earnshaw, W.C. (2008). Molecular and genetic analysis of condensin function in vertebrate cells. *Mol. Biol. Cell* **19**, 3070–3079.
- Kappel, C., Zachariae, U., Dölker, N., and Grubmüller, H. (2010). An unusual hydrophobic core confers extreme flexibility to HEAT repeat proteins. *Biophys. J.* **99**, 1596–1603.
- Kimura, K., and Hirano, T. (1997). ATP-dependent positive supercoiling of DNA by 13S condensin: a biochemical implication for chromosome condensation. *Cell* **90**, 625–634.
- Kimura, K., and Hirano, T. (2000). Dual roles of the 11S regulatory subcomplex in condensin functions. *Proc. Natl. Acad. Sci. USA* **97**, 11972–11977.
- Lee, J., Ogushi, S., Saitou, M., and Hirano, T. (2011). Condensins I and II are essential for construction of bivalent chromosomes in mouse oocytes. *Mol. Biol. Cell* **22**, 3465–3477.
- Lewis, C.D., and Laemmli, U.K. (1982). Higher order metaphase chromosome structure: evidence for metalloprotein interactions. *Cell* **29**, 171–181.
- Maeshima, K., Hihara, S., and Eltsov, M. (2010). Chromatin structure: does the 30-nm fibre exist in vivo? *Curr. Opin. Cell Biol.* **22**, 291–297.
- Nasmyth, K., and Haering, C.H. (2005). The structure and function of SMC and kleisin complexes. *Annu. Rev. Biochem.* **74**, 595–648.
- Neuwald, A.F., and Hirano, T. (2000). HEAT repeats associated with condensins, cohesins and other chromosome-related complexes. *Genome Res.* **10**, 1445–1452.
- Ohsumi, K., Katagiri, C., and Kishimoto, T. (1993). Chromosome condensation in *Xenopus* mitotic extracts without histone H1. *Science* **262**, 2033–2035.
- Onn, I., Aono, N., Hirano, M., and Hirano, T. (2007). Reconstitution and subunit geometry of human condensin complexes. *EMBO J.* **26**, 1024–1034.
- Ono, T., Losada, A., Hirano, M., Myers, M.P., Neuwald, A.F., and Hirano, T. (2003). Differential contributions of condensin I and condensin II to mitotic chromosome architecture in vertebrate cells. *Cell* **115**, 109–121.
- Paulson, J.R., and Laemmli, U.K. (1977). The structure of histone-depleted metaphase chromosomes. *Cell* **12**, 817–828.
- Piazza, I., Rutkowska, A., Ori, A., Walczak, M., Metz, J., Pelechano, V., Beck, M., and Haering, C.H. (2014). Association of condensin with chromosomes depends on DNA binding by its HEAT-repeat subunits. *Nat. Struct. Mol. Biol.* **21**, 560–568.
- Saitoh, N., Goldberg, I.G., Wood, E.R., and Earnshaw, W.C. (1994). Scll: an abundant chromosome scaffold protein is a member of a family of putative ATPases with an unusual predicted tertiary structure. *J. Cell Biol.* **127**, 303–318.
- Savvidou, E., Cobbe, N., Steffensen, S., Cotterill, S., and Heck, M.M.S. (2005). *Drosophila* CAP-D2 is required for condensin complex stability and resolution of sister chromatids. *J. Cell Sci.* **118**, 2529–2543.
- Schleiffer, A., Kaitna, S., Maurer-Stroh, S., Glotzer, M., Nasmyth, K., and Eisenhaber, F. (2003). Kleisins: a superfamily of bacterial and eukaryotic SMC protein partners. *Mol. Cell* **11**, 571–575.
- Shintomi, K., and Hirano, T. (2011). The relative ratio of condensin I to II determines chromosome shapes. *Genes Dev.* **25**, 1464–1469.
- Shintomi, K., Iwabuchi, M., Saeki, H., Ura, K., Kishimoto, T., and Ohsumi, K. (2005). Nucleosome assembly protein-1 is a linker histone chaperone in *Xenopus* eggs. *Proc. Natl. Acad. Sci. USA* **102**, 8210–8215.
- St-Pierre, J., Douziech, M., Bazile, F., Pascariu, M., Bonnell, E., Sauvé, V., Ratsima, H., and D'Amours, D. (2009). Polo kinase regulates mitotic chromosome condensation by hyperactivation of condensin DNA supercoiling activity. *Mol. Cell* **34**, 416–426.
- Sutani, T., and Yanagida, M. (1997). DNA renaturation activity of the SMC complex implicated in chromosome condensation. *Nature* **388**, 798–801.
- Tedeschi, A., Wutz, G., Huet, S., Jaritz, M., Wuensche, A., Schirghuber, E., Davidson, I.F., Tang, W., Cisneros, D.A., Bhaskara, V., et al. (2013). Wapl is an essential regulator of chromatin structure and chromosome segregation. *Nature* **501**, 564–568.